

Online RIS Configuration Learning for Arbitrary Large Numbers of 1-Bit Phase Resolution Elements

Kyriakos Stylianopoulos and George C. Alexandropoulos

Department of Informatics and Telecommunications, National and Kapodistrian University of Athens

Panepistimiopolis Ilissia, 15784 Athens, Greece

emails: {kstylianop, alexandg}@di.uoa.gr

Abstract—Reinforcement Learning (RL) approaches are lately deployed for orchestrating wireless communications empowered by Reconfigurable Intelligent Surfaces (RISs), leveraging their online optimization capabilities. Most commonly, in RL-based formulations for realistic RISs with low resolution phase-tunable elements, each configuration is modeled as a distinct reflection action, resulting to inefficient exploration due to the exponential nature of the search space. In this paper, we consider RISs with 1-bit phase resolution elements, and model the action of each of them as a binary vector including the feasible reflection coefficients. We then introduce two variations of the well-established Deep Q-Network (DQN) and Deep Deterministic Policy Gradient (DDPG) agents, aiming for effective exploration of the binary action spaces. For the case of DQN, we make use of an efficient approximation of the Q-function, whereas a discretization post-processing step is applied to the output of DDPG. Our simulation results showcase that the proposed techniques greatly outperform the baseline in terms of the rate maximization objective, when large-scale RISs are considered. In addition, when dealing with moderate scale RIS sizes, where the conventional DQN based on configuration-based action spaces is feasible, the performance of the latter technique is similar to the proposed learning approach.

Index Terms—Reconfigurable intelligent surfaces, binary action space, deep reinforcement learning, phase configuration.

I. INTRODUCTION

The technology of Reconfigurable Intelligent Surfaces (RISs) has been acknowledged as one of the key ingredients of next 6-th Generation (6G) of wireless networks [1]. Those surfaces consist of potentially large numbers of nearly passive (i.e., without any power amplification) meta-material elements that induce a phase shift to the propagating wireless signals, depending on their internal generalized reflection states [2]. The overall RIS configuration can be intelligently controlled, therefore empowering the wireless environment with dynamic reconfiguration abilities that offer unprecedented benefits in terms of performance indicators and provided services [3].

To fully realize the potential of RISs [4], however, their phase configurations need to be carefully selected to serve the underlying system objective. As a result, the problem of phase tuning has been extensively studied using either conventional optimization schemes (e.g., [5], [6]), or techniques stemming from Machine Learning (ML) [7], [8]. A distinct sub-domain of the latter, called Deep Reinforcement Learning (DRL) is especially designed for solving online decision problems using learning algorithms that are trained through continuous interactions within a controllable environment. DRL methods

targeting RIS control cover a great variety of design objectives, including energy efficiency [9], resource scheduling [10], [11], and secrecy rate [12]. However, the principal utilization of such Artificial Intelligence (AI)-based orchestrators is for increased spectral efficiency through combinations of analog (RIS) and analog/digital (transmit/receive) beamforming [13]–[18], alongside other considerations such as power allocation [19] or Unmanned Autonomous Vehicle (UAV) control [20].

In this paper, we are concerned with the problem of configuring RISs that are consisted of large numbers of individually controllable unit-elements through DRL orchestration. Future wireless environments are envisioned to deploy multiple operating metasurfaces [3], each one comprised of hundreds or thousands of phase-tunable elements. At the same time, current RIS prototypes are predominantly designed with 1-bit quantized phase shifts per element [2], [21], leading to (base-2) exponential numbers of available RIS configurations. In general, DRL agents that are tasked with selecting the discrete phase shifts, treat each of the possible configurations as an individual action (e.g., [16], [17]) and their training process involves receiving feedback on the selected profile at every iteration. As a result, such algorithms are prone to inefficient search-space-exploration and slow convergence rate due the rapid increase of the cardinality of the action space. Motivated by the fact that for 1-bit phase-quantized RISs, each element’s action can be represented by a binary vector, so that each vector element denotes the selection of one of the two available phase shifts, we devised two modified versions of the celebrated DRL algorithms Deep Q-Network (DQN) and Deep Deterministic Policy Gradient (DDPG), which leverage the binary decomposition of the RIS configurations, resulting in both cases to an action space that is linear to the number of RIS elements. This is amenable to tuning each element individually, which leads to a more efficient propagation of feedback information, compared to treating each available overall RIS configuration as an individual action.

The rest of the paper is structured as follows: Section II describes the considered system setup and operation objective, whereas Section III includes the paper’s DRL formulation and presents the proposed modified versions of the DQN and DDPG algorithms. These algorithms are numerically evaluated in Section IV, while Section V contains a discussion on the proposed methodology, followed by the paper’s conclusion in Section VI.

Notation: Bold-faced small and capital letters denote vectors and matrices, respectively, while calligraphy typeface denotes sets. $[x]_i$ denotes the i -th element of x . The cardinality

This work has been supported by the EU H2020 RISE-6G project under grant number 10101701.

of a set \mathcal{S} is expressed as $\text{card}(\mathcal{S})$, the $\text{vec}(\cdot)$ operator vectorizes a matrix in row format, and $\text{diag}(\mathbf{x})$, for an n -dimensional vector \mathbf{x} , creates an $n \times n$ matrix with the elements of \mathbf{x} placed along the main diagonal. The expectation operation is expressed as $\mathbb{E}\{\cdot\}$ and $\text{Real}\{\cdot\}$ ($\text{Imag}\{\cdot\}$) returns the real (imaginary) part of a complex quantity. Finally, $j \triangleq \sqrt{-1}$.

II. SYSTEM MODEL AND DESIGN OBJECTIVE

In this section, we give a description of the system model that will be considered during the presentation of the DRL methods and the numerical evaluation. Since the aim of this paper is to examine the performance of ML-based controllers with large-scale RISs, we have purposely selected a simple system architecture for clarity. More complex system architectures will be studied in the journal version of this work. We assume a Multiple-Input Single-Output (MISO) downlink communication wireless environment that includes a Base Station (BS) equipped with K antennas and a single-antenna User Equipment (UE) which remains at a fixed location. The presence of a blocker is assumed to obstruct the direct link between them. Instead, the communication is enabled by the positioning of an RIS consisted of N controllable phase shifting elements. As is typical in the industry [2], [21], we consider a metasurface structure, in which the state φ_i of each unit meta-element i ($1 \leq i \leq N$) can be set to one out of two predefined phases, say ϑ_1 and ϑ_2 . The configuration space of the RIS can thus be defined as $\mathcal{F} = \{\vartheta_1, \vartheta_2\}^N$ with $\text{card}(\mathcal{F}) = 2^N$. Let $\boldsymbol{\phi} \triangleq [\exp(j\pi\varphi_1), \dots, \exp(j\pi\varphi_N)]^T$ denote the configuration vector of the RIS and let $\boldsymbol{\Phi} \triangleq \text{diag}(\boldsymbol{\phi}) \in \mathbb{C}^{N \times N}$. By further denoting with $\mathbf{H} \in \mathbb{C}^{K \times N_T}$ and $\mathbf{g} \in \mathbb{C}^{1 \times N}$ the channel gain matrices for the BS-RIS and RIS-UE wireless links, respectively, the baseband received signal at the UE can be expressed as

$$y = \mathbf{g}\boldsymbol{\Phi}\mathbf{H}\mathbf{v}x + \tilde{n}, \quad (1)$$

where \tilde{n} models the Additive White Gaussian Noise (AWGN) with zero mean and variance σ^2 , x is the symbol transmitted with power P , and $\mathbf{v} \in \mathbb{C}^{N_T \times 1}$ represents the BS precoding vector. To focus specifically on the RIS phase configuration control in this paper, we do not consider the design and selection of the precoder as part of the problem formulation, even though it constitutes an important aspect of wireless systems with many DRL-based methods considering joint analog and digital beamforming [13]–[16]. To this end, we simply set each element of vector \mathbf{v} to $1/K$ to obtain a unit power precoding vector.

To access the quality of the considered communication system, the instantaneous Signal-to-Noise Ratio (SNR) performance is defined as (the involved channel matrices need to be perfectly known) $\gamma \triangleq \frac{P}{\sigma^2} |\mathbf{g}\boldsymbol{\Phi}\mathbf{H}|^2$. Finally, we formulate the optimization objective of the achievable rate performance per unit bandwidth as a function of the controllable RIS configuration and the channel state matrices:

$$\begin{aligned} \mathcal{OP} : \quad & \max_{\boldsymbol{\phi}} R_{\mathbf{g},\mathbf{H}}(\boldsymbol{\phi}) \triangleq \log_2 \left(1 + \frac{P}{\sigma^2} |\mathbf{g}\boldsymbol{\Phi}\mathbf{H}|^2 \right) \\ & \text{s.t.} \quad \varphi_i \in \mathcal{F}, \quad 1 \leq i \leq N. \end{aligned}$$

In this problem formulation, we make the following assumptions: *i* The channel realizations through time are Independent and Identically Distributed (IID); *ii* The UE is capable of measuring the received SNR, and consequently, share this measure with the RIS controller; *iii* The controller has complete Channel State Information (CSI) knowledge and is capable of changing the configuration of the RIS without delay; and *iv* Similarly, the communication between the controller and the network's nodes is assumed to have negligible effect. The problem of practical channel estimation [2] and its effect on orchestrating RISs lies out of the primary focus of this paper.

III. PROPOSED DRL-BASED RIS CONFIGURATION

A. Reinforcement Learning Formulation

The Reinforcement Learning (RL) methodology involves a computationally-enabled agent (i.e., the RIS controller) interacting with an environment (i.e., the RIS-enabled communication system) in order to maximize its own goal. Concretely, at every discrete time step t , the agent, upon acquiring an observation from the environment, is tasked with the selection of one of the available actions. The action affects the internal state of the environment and the latter, in turn, gives off a reward signal to the agent, while moving to the next state. To formulate an RL problem that is equivalent to the design objective in \mathcal{OP} within a finite time horizon, we next define the individual components of the corresponding Markov Decision Process (MDP):

- **Observation (state):** We assume that CSI is available to the RIS controller, thus the observation vector is consisted of the elements of the two channel matrices: $\mathbf{s}_t \triangleq [\text{vec}(\mathbf{H}_t), \text{vec}(\mathbf{g}_t)]^t \in \mathbb{C}^{K(N+1)}$. Note that the actual implementations of the DRL algorithms are not designed to process complex values, as a result the actual observation vector is constructed as $\hat{\mathbf{s}}_t \triangleq [\text{Real}(\mathbf{s}_t^T), \text{Imag}(\mathbf{s}_t^T)]^T$.
- **Action:** The agent controls the configuration of the RIS by selecting a vector \mathbf{a}_t with elements in $\{0, 1\}^N$, so that $[\mathbf{a}_t]_i$ sets the phase shift of the i -th ($1 \leq i \leq N$) RIS unit element to either of the two predefined phases.
- **Reward:** The selected RIS phase configuration is used, which along with the current channel matrix realizations, results in the instantaneous SNR measurement at the UE's end. The achievable rate serves as the reward at each discrete time instant t : $r_t \triangleq R_{\mathbf{g},\mathbf{H}}(\boldsymbol{\phi})$.
- **Transition:** At the time $t + 1$, the wireless environment proceeds to the next state by sampling IID channel realizations as \mathbf{g}_{t+1} and \mathbf{H}_{t+1} .

The aim of the agent is to maximize the (undiscounted) expected sum of rewards, i.e., $\mathbb{E} \left\{ \sum_{t=1}^T r_t \right\}$, for some final time horizon T . In the previous expression, the expectation is taken with respect to the transition probability distribution.

In the following sections, we proceed under the proposed MDP framework to present the modified versions of two DRL algorithms, which are named *bin-DQN* and *bin-DDPG*, respectively. For brevity, only the components that are relevant to the proposed modifications are described, omitting

implementation details and theoretical understanding to future versions of this work.

B. bin-DQN

Q-Learning is a method for solving an MDP by finding a (stochastic) policy ϖ^* (i.e., action-selection function) that maximizes the following state-action value function:

$$Q(s, \mathbf{a}) \triangleq \mathbb{E} \left\{ \sum_{t=1}^T r_t \mid \mathbf{s}_1 = s, \mathbf{a}_1 = \mathbf{a} \right\}. \quad (2)$$

The optimal policy results in a Q-function that is maximal for every state-action pair, and for a given state s' it selects the action $\mathbf{a}' = \operatorname{argmax} Q(s', \mathbf{a})$. The Deep Q-Network (DQN) algorithm [22] approximates (2) by a neural network $Q_w(s, \mathbf{a})$, with vector \mathbf{w} representing its weights, that receives an observation as input and outputs the predicted Q value for each action. The network is trained using Stochastic Gradient Descent (SGD) on the Temporal Difference (TD) error function (given the experience samples (s, \mathbf{a}, r, s'))

$$L(\mathbf{w}) = \frac{1}{2} \left(r + \max_{\hat{\mathbf{a}}} Q_w(s', \hat{\mathbf{a}}) - Q_w(s, \mathbf{a}) \right)^2, \quad (3)$$

where s' denotes the successor state of s as observed by the agent. Note that the time and space complexities for selecting an action for the above process is $O(2^N)$, since the network includes one output neuron for each distinct action, i.e., each RIS phase configuration.

Having defined each action in the previous section as an N -element vector with binary elements, in this work, we adopt the neural network architecture proposed in [23] that approximates the state-action function as follows:

$$Q_w(s, \mathbf{a}) = q_w^0(s) + \sum_{i=1}^N [\mathbf{a}]_i [\mathbf{q}_w(s)]_i = q_w^0(s) + \mathbf{a}^T \mathbf{q}_w(s). \quad (4)$$

The neural network in this expression has two distinct output layers, namely, $q_w^0(s) \in \mathbb{R}$ and $\mathbf{q}_w(s) \in \mathbb{R}^{N \times 1}$. It is noted that the dot product operation on the right-hand side of (4) can be seen as a per-element activation/suppression filter on the partial output of the network. For a given state, the selected action can be derived as:

$$[\mathbf{a}]_i = \begin{cases} 1, & [\mathbf{q}_w(s)]_i > 0 \\ 0, & \text{otherwise} \end{cases}, \quad i = 1, 2, \dots, N. \quad (5)$$

Clearly, the action selected by (5) is the one maximizing (4) at the given state, since all positive elements of $\mathbf{q}_w(s)$ are activated and contribute to the summation, while the negative values are suppressed. The architecture is illustrated in Fig 1. Using this approximate form, the space and time complexities of this variation are reduced to $O(N)$, which are tractable to a greater extent, when considering the practical deployment of those algorithms in autonomous wireless systems with potentially limited computational infrastructures. Let it be noted that (4) remains a differentiable function with respect to \mathbf{w} , meaning that the gradient steps and backpropagation can be applied as normal under this form.

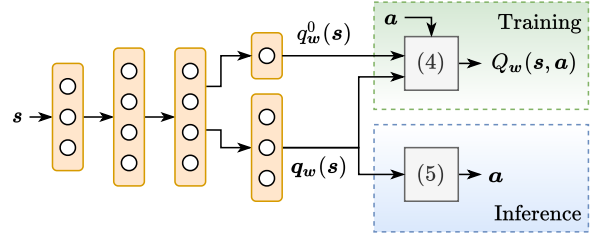


Fig. 1. Schematic diagram of the Q-function approximation network of [23]. The action is determined by the use of $[\mathbf{q}_w(s)]_i$ via (5), whereas both output layers are utilized to compute $Q_w(s, \mathbf{a})$ through (4) during training updates. This architecture assumes that \mathbf{a} 's elements take binary values.

C. bin-DDPG

While DQN has exhibited increased popularity, its domain of application is constrained to problems with discrete action spaces. MDPs, whose action space is continuous, require special treatment, since it is not straightforward to compute the value function in the continuous domain. Conversely, algorithms of this category are probably better equipped to deal with vector-type actions, since it is typical to employ policy networks that are trained to predict the exact value of each element of the optimal action vector at every time step. As a result, their output value – when considering the existing MDP formulation – is already shaped as an N -element vector. This fact can be exploited to allow for their application in this paper's binary-vector domain, by simply applying a discretization step to turn the continuous values for each element to a binary one. Concretely, suppose $\varpi_{w'}(s) \in \mathbb{R}^{N \times 1}$ denotes the output vector of a policy network when observing state s . Then, the selected action vector can be constructed as:

$$[\mathbf{a}]_i = \begin{cases} 1, & [\varpi_{w'}(s)]_i > 0 \\ 0, & \text{otherwise} \end{cases}, \quad i = 1, 2, \dots, N, \quad (6)$$

which resembles the action selection operation of bin-DQN. In our numerical evaluation in the next section, we will use the predominant Deep Deterministic Policy Gradient (DDPG) algorithm [24], upon applying (6) to the output of its policy network. Note that this modification is completely *transparent* to the underlying agent and it requires no modifications nor assumptions, apart from the fact that the co-domain of the activation function of the final layer of the policy network contains both positive and negative values, which is readily satisfied by choosing \tanh as the network's activation function.

IV. SIMULATION RESULTS

A. Simulation Setup

In our simulation setup, we consider the BS placed at the 3D Cartesian coordinates $(10, 5, 2)$, the UE at $(8.7, 14.4, 1.6)$, and the RIS at $(7.5, 13, 2)$. The surface is assumed to be oriented parallel to the y - z plane. The predefined RIS phase states per elements are set to $\vartheta_1 = 0$ and $\vartheta_2 = \pi$. The BS is operating at the carrier frequency 5 GHz with transmit power 40 dBm. Additionally, σ^2 is set to -100 dBm, and the free space pathloss model is used for computing the attenuation of the channels. The channel coefficients exhibit Ricean fading with

TABLE I
HYPER-PARAMETER VALUES OF THE CONSIDERED DRL ALGORITHMS.

Parameter Value	DQN	bin-DQN	bin-DDPG
Value network learning rate	0.001	0.01	0.001
Policy network learning rate	-	-	0.0001
Batch size	128	128	64
ϵ -greedy	0.1	0.1	-
Gradient clipping range	(-1, 1)	(-1, 1)	-
Target update period	1000	2000	1
Target soft update temperature	0.18	0.05	0.00001
Ornstein-Uhlenbeck μ	-	-	0
Ornstein-Uhlenbeck θ	-	-	0.15
Neural network component	DQN	bin-DQN	bin-DDPG
Convolutional layers		2	-
Units per layer		64	-
Kernel width per layer		5	-
Max pool layers		2	-
Kernel width per layer		5	-
Fully connected layers		5	3
Units per layer		100	400
Dropout probability		0.2	0.2
Activation functions		ReLU, tanh	ReLU, tanh

a dominant direct path; specifically, the Ricean factors for all involved channels were set to 30 dB. A complete description of the channel model is given in [16].

B. Evaluation Process

The two modified agents, presented in Section III, are tasked to solve \mathcal{OP} , by training in the described MDP. The two approaches are compared against the original version of the DQN algorithm, along with the random RIS configuration baseline, and the optimal configuration selection strategy, the latter serving as an upper bound. The optimal selection is implemented, when possible, by exhaustively searching all possible configurations for a given channel state.

The agents are trained for 10000 time steps (i.e., channel realizations). Since algorithms learn in an off-policy manner (i.e., they purposely select sub-optimal actions at random for better exploration, which provides a lower bound of their true performance), their performance is evaluated at the end of the training process for 1500 channel transitions, in which the agents act using their (greedy) learned policy. The baseline and the optimal strategy are evaluated during the same period. The results, presented below, show the mean rewards (achievable rates) over the evaluation steps. Given the plurality of the considered DRL methods and setup instances, we have refrained from performing an extensive hyper-parameter tuning or employing advanced neural network architectures. The chosen parameter values are given in Table I. The simulations were performed on a desktop computer with 11-th generation Intel Core i7 CPU, 32GB RAM, and an Nvidia RTX 3080 (10GB VRAM) GPU. The code was implemented using PyTorch and Tensorflow.

C. Achievable Rate Evaluation

The achievable rate of the proposed DRL algorithms and the benchmark techniques versus the number N of RIS elements are depicted in Figs 2 and 3. Due to the exponential increase of both the time complexity of the exhaustive search and the space complexity of the original DQN approach, the computations involved rapidly become intractable. To account for that, we split the comparison process into two instances.

In Fig 2, we foremost consider N values up to 110. In addition, we group $N_{\text{group}} = 5$ consecutive RIS elements together, so that elements within the same group share the same reflection phase. Thus, the cardinality of the action space for a given value of N becomes $2^{N/N_{\text{group}}}$. Additionally, note that in order to attain a more extensive collection of evaluation points, we did not constraint the RIS elements to be perfect squares, and as a result, the planar RISs in the simulation have arbitrary rectangular shapes. Those two modifications affect the behavior of the system under examination, resulting in lower achievable rates with fluctuations in very small RIS sizes. To better investigate the effectiveness of the algorithms in large-scale RISs, we repeat the evaluation process for all perfect square N values up to 1500 in Fig 3. In this figure, only the proposed bin-DQN and bin-DDPG algorithms are displayed, along with the random baseline, since it is infeasible to run exhaustive search or DQN. To account for the enlarged action spaces, we allow the DRL algorithms to be trained for 20000 time steps; no elements' grouping was applied in that case.

It can be observed from Fig 2 that the performance of the proposed techniques is on par with the state-of-the-art DQN algorithm for low-to-moderate RIS sizes. In particular, their performance is close to the optimal achievable rate in the initial toy examples, and at the same time it does not substantially drop, when compared to the naive random RIS configuration selection. The results in Fig 3 showcase that the achievable rates of the randomly configured surface decrease exponentially, which corroborates the need for intelligent configuration techniques in order to benefit from the RIS technology. Interestingly, it is depicted that both proposed DRL agents offer gains in the achievable rate that are double to triple with respect to the random baseline in moderate-to-large RIS sizes (i.e., up to $N = 500$). However, the trend in the performance is decreasing, indicating that while effective, the performance of those techniques can be improved. Especially for the case of bin-DQN, it is observed that the drop on its achievable rate is more abrupt, reducing to essentially random action selection for $N > 600$. On the other hand, the discretized modification of DDPG continues to exhibit an important improvement over the baseline even for the largest N values, although its behavior is less stable.

V. LIMITATIONS AND FUTURE WORK

The performance results in the previous section concern agents incorporating relatively small neural networks in large action and observation spaces (e.g., for $N = 1500$, the networks receive 15000-dimensional state vectors as inputs) and the training periods were restrained to allow for multiple trials to take place. This is one possible explanation for the general decreasing trend and the fluctuations on DDPG's performance. At the same time, it is clear that the Q-function approximation adopted here is reasonable up to a certain extend. A potential extension of this work is to devise a different kind of approximation for the action-state function, that still retains the $O(N)$ complexity, while being tailored to the system modeling details; this direction naturally leads to some variations of deep unfolding [25].

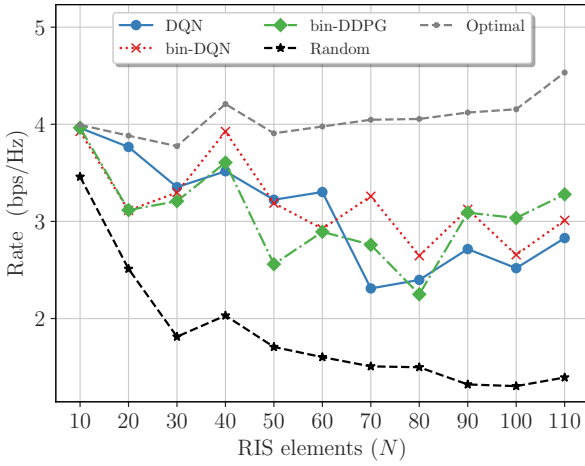


Fig. 2. Achievable rates versus N for the proposed bin-DQN and bin-DDPG in low-to-moderate RIS-sized systems. The original DQN, the (optimal) exhaustive search, and the random configuration are used as baselines.

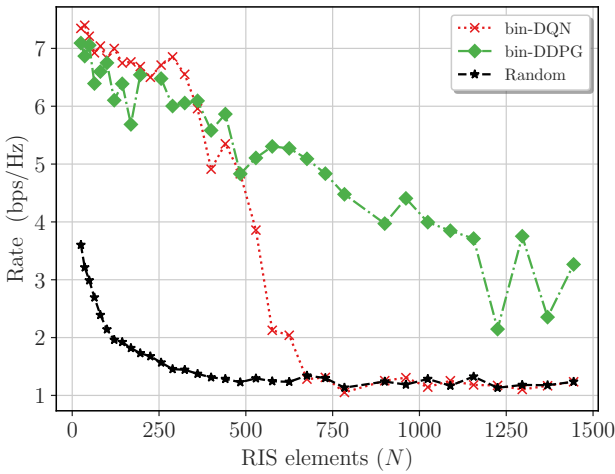


Fig. 3. Achievable rates versus N for the proposed bin-DQN and bin-DDPG algorithms in moderate-to-large RIS-sized systems, compared to the random baseline selection.

As discussed earlier, a simplified wireless system has been considered. In practical applications, it is reasonable to assume other free parameters (e.g., precoding selection and power allocation), while having limited CSI availability, and intricate network components. Such cases have been covered in the literature often by employing the original versions of the DQN and DDPG algorithms. It is thus our viewpoint that the proposed neural networks can be incorporated as parts of extended purpose agents, with more elaborate Multiple-Input Multiple-Output (MIMO)-inspired neural network architectures.

VI. CONCLUSION

Current state-of-the-art DRL approaches suffer from the exponential increase of the action space when large-scale RISs with quantized phases are employed. Our proposed formulation considered 1-bit resolution phases which allows for the configurations to be viewed as binary-element vectors. Under this viewpoint, we have presented neural network architectures extensions. For the case of DQN, an activation/suppression Q-function approximation was adopted, whereas DDPG's output was discretized. Our simulation results showcased efficient configuration of arbitrary-scale RISs, while providing comparable performance with the considered benchmark approaches.

REFERENCES

- [1] E. Calvanese Strinati *et al.*, "Wireless environment as a service enabled by reconfigurable intelligent surfaces: The RISE-6G perspective," in *Proc. Joint EuCNC & 6G Summit*, Porto, Portugal, Jun. 2021.
- [2] M. Jian *et al.*, "Reconfigurable intelligent surfaces for wireless communications: Overview of hardware designs, channel models, and estimation techniques," 2022, [Online] <https://arxiv.org/pdf/2203.03176.pdf>.
- [3] E. Calvanese Strinati *et al.*, "Reconfigurable, intelligent, and sustainable wireless environments for 6G smart connectivity," *IEEE Commun. Mag.*, vol. 59, no. 10, pp. 99–105, Oct. 2021.
- [4] G. C. Alexandropoulos *et al.*, "Reconfigurable intelligent surfaces and metamaterials: The potential of wave propagation control for 6G wireless communications," *IEEE ComSoc TCCN Newslett.*, vol. 6, no. 1, pp. 25–37, Jun. 2020.
- [5] Z. Peng *et al.*, "Analysis and optimization for RIS-aided multi-pair communications relying on statistical CSI," *IEEE Trans. Veh. Technol.*, vol. 70, pp. 3897–3901, Apr. 2021.
- [6] X. Cheng *et al.*, "Joint optimization for RIS-assisted wireless communications: From physical and electromagnetic perspectives," *IEEE Trans. Commun.*, vol. 70, no. 1, pp. 606–620, Jan. 2022.
- [7] G. C. Alexandropoulos, S. Samarakoon, M. Bennis, and M. Debbah, "Phase configuration learning in wireless networks with multiple reconfigurable intelligent surfaces," in *Proc. IEEE GLOBECOM*, Taipei, Taiwan, Dec. 2020.
- [8] S. Zhang *et al.*, "AIRIS: Artificial intelligence enhanced signal processing in reconfigurable intelligent surface communications," *China Commun.*, vol. 18, no. 7, pp. 158–171, 2021.
- [9] G. Lee *et al.*, "Deep reinforcement learning for energy-efficient networking with reconfigurable intelligent surfaces," in *Proc. IEEE ICC*, Dublin, Ireland, Jun. 2020.
- [10] X. Gao *et al.*, "Machine learning empowered resource allocation in IRS aided MISO-NOMA networks," 2021, [Online] <https://arxiv.org/pdf/2103.11791.pdf>.
- [11] A. Al-Hilo *et al.*, "Reconfigurable intelligent surface enabled vehicular communication: Joint user scheduling and passive beamforming," 2021, [Online] <https://arxiv.org/pdf/2101.12247.pdf>.
- [12] H. Yang *et al.*, "Deep reinforcement learning-based intelligent reflecting surface for secure wireless communications," *IEEE Trans. Wireless Commun.*, vol. 20, no. 1, pp. 375–388, Jan. 2021.
- [13] A. Taha *et al.*, "Deep reinforcement learning for intelligent reflecting surfaces: Towards standalone operation," in *Proc. IEEE SPAWC*, Atlanta, USA, May 2020.
- [14] C. Huang *et al.*, "Reconfigurable intelligent surface assisted multiuser MISO systems exploiting deep reinforcement learning," *IEEE J. Sel. Areas Commun.*, vol. 38, no. 8, pp. 1839–1850, Aug. 2020.
- [15] K. Feng *et al.*, "Deep reinforcement learning based intelligent reflecting surface optimization for MISO communication systems," *IEEE Wireless Commun. Lett.*, vol. 9, no. 5, pp. 745–749, May 2020.
- [16] K. Stylianopoulos *et al.*, "Deep contextual bandits for orchestrating multi-user MISO systems with multiple RISs," in *IEEE ICC*, Seoul, South Korea, May 2022, [Online] <https://arxiv.org/pdf/2202.08194.pdf>.
- [17] C. Huang *et al.*, "Multi-hop RIS-empowered terahertz communications: A DRL-based hybrid beamforming design," *IEEE J. Sel. Areas Commun.*, vol. 39, no. 6, pp. 1663–1677, Jun. 2021.
- [18] J. Kim *et al.*, "Multi-IRS-assisted multi-cell uplink MIMO communications under imperfect CSI: A deep reinforcement learning approach," 2021, [Online] <https://arxiv.org/pdf/2011.01141.pdf>.
- [19] X. Liu *et al.*, "RIS enhanced massive non-orthogonal multiple access networks: Deployment and passive beamforming design," *IEEE J. Sel. Areas Commun.*, vol. 39, no. 4, pp. 1057–1071, Apr. 2021.
- [20] M. Samir *et al.*, "Optimizing age of information through aerial reconfigurable intelligent surfaces: A deep reinforcement learning approach," *IEEE Trans. Veh. Technol.*, vol. 70, no. 4, pp. 3978–3983, Apr. 2021.
- [21] G. C. Alexandropoulos *et al.*, "Reconfigurable intelligent surfaces for rich scattering wireless communications: Recent experiments, challenges, and opportunities," *IEEE Commun. Mag.*, vol. 59, no. 6, pp. 28–34, Jun. 2021.
- [22] V. Mnih *et al.*, "Human-level control through deep reinforcement learning," *Nature*, vol. 518, no. 7540, pp. 529–533, 2015.
- [23] N. Yoshida, "Q-networks for binary vector actions," 2015, [Online] <https://arxiv.org/pdf/1512.01332.pdf>.
- [24] T. Lillicrap *et al.*, "Continuous control with deep reinforcement learning," 2016, [Online] <https://arxiv.org/pdf/1509.0297.pdf>.
- [25] A. Balatsoukas-Stimming *et al.*, "Deep unfolding for communications systems: A survey and some new directions," in *Proc. IEEE SIPS*, Nanjing, China, Oct. 2019, pp. 266–271.